International Journal of Chronic Obstructive Pulmonary Disease Dovepress
open access to scientific and medical research

Open Access Full Text Article

ORIGINAL RESEARCH

Protective Effect of the Total Alkaloid Extract from Bulbus *Fritillariae pallidiflorae* in a Mouse Model of Cigarette Smoke-Induced Chronic Obstructive Pulmonary Disease

Xiaoyu Wang[1], Er-Bu AGA[2], Wai Ming Tse[3], Kathy Wai Gaun Tse[3], Bengui Ye[1,2]

[1]Key Laboratory of Drug-Targeting and Drug Delivery System of the Education Ministry, Sichuan Engineering Laboratory for Plant-Sourced Drug and Sichuan Research Center for Drug Precision Industrial Technology, West China School of Pharmacy, Sichuan University, Chengdu, Sichuan, 610041, People's Republic of China; [2]Medical College of Tibet University, Lasa, Tibet, 850002, People's Republic of China; [3]Nin Jiom Medicine Manufactory (H. K.) Limited, Hong Kong, 999077, People's Republic of China

Correspondence: Bengui Ye, West China School of Pharmacy, Sichuan University, Chengdu, 610041, People's Republic of China, Fax +86-28-85503950, Email benguiye513@163.com

Purpose: In recent years, the incidence of chronic obstructive pulmonary disease (COPD) has been increasing year by year, but therapeutic drugs has no breakthrough. The total alkaloid extract from Bulbus *Fritillariae pallidiflorae* (BFP-TA) is widely used in treating lung diseases. Therefore, this study aimed to investigate the protective effect and mechanism of BFP-TA in COPD mice.

Methods: BFP-TA was prepared by macroporous adsorbent resin, and the material basis of BFP-TA was analyzed by HPLC-ELSD and UHPLC-MS/MS. Then, the COPD mouse model was induced by cigarette smoke (CS) for 12 weeks, administered at weeks 9–12. Subsequently, the body weight, lung-body ratio, pulmonary function, histopathology, and the levels of pro-inflammatory cytokines, matrix metalloproteinases (MMPs) and oxidative stress markers in the serum of mice were determined. The expressions of related protein of EMT and MAPK signaling pathways in the lung tissues of mice were detected by Western blot.

Results: The alkaloid relative content of BFP-TA is 64.28%, and nine alkaloids in BFP-TA were identified and quantified by UHPLC-MS/MS. Subsequently, the animal experiment showed that BFP-TA could improve pulmonary function, and alleviate inflammatory cell infiltration, pulmonary emphysema, and collagen fiber deposition in the lung of COPD mice. Furthermore, BFP-TA could decrease the levels of pro-inflammatory cytokines (TNF-α, IL-6 and IL-1β), MMPs (MMP-9 and MMP-12) and MDA, while increase the levels of TIMP-1 and SOD. Moreover, BFP-TA could decrease the protein expressions of collagen I, vimentin, α-SMA, MMP-9, MMP-9/TIMP-1, Bax, p-JNK/JNK, p-P38/P38, and p-ERK/ERK, while increase the level of E-cadherin.

Conclusion: This study is the first to demonstrate the protective effect of BFP-TA in CS-induced COPD mouse model. Furthermore, BFP-TA may improve airway remodeling by inhibiting the EMT process and potentially exert anti-inflammatory effect by inhibiting the MAPK signaling pathway.

Keywords: Bulbus *Fritillariae pallidiflorae*, total alkaloid, COPD, EMT, MAPK

Introduction

Chronic obstructive pulmonary disease (COPD) is a disease characterized by restricted and incompletely reversible airflow, inflammation of the lungs, and the destruction of emphysema.[1] There are two main phenotypes: the airway phenotype, characterized by chronic obstructive bronchitis; and the emphysematous phenotype, characterized by reduced gas exchange area and exercise capacity.[2] Based on a report released by the World Health Organization in 2020,[3] COPD has become the third leading cause of death in the world, and the fatality rate is increasing every year. COPD is usually caused by regular exposure to smoking, toxic gases, dust particles, etc.,[4,5] among which smoking is recognized as the most important factor contributing to COPD and irreversible airflow

Received: 11 January 2024
Accepted: 20 May 2024
Published: 10 June 2024

limitations. The pathogenesis of COPD is complex, currently, the recognized pathogenic mechanisms include chronic inflammation, oxidative stress, protease/anti-protease imbalance, airway remodeling, apoptosis, decreased immunity, etc., and the pathogenesis of COPD is caused by combination of multiple mechanisms.[6–8]

Although basic research on COPD has many achievements, the pathogenesis of COPD has not been fully elucidated, and there has no breakthrough in therapeutic drugs. Therapeutic interventions for COPD focus on improving lung function, symptoms, quality of life, and reducing disease progression rather than the risk of death.[9] Currently, bronchodilators (such as β2 agonists, anticholinergics, and theophyllines), glucocorticoids, and phosphodiesterase inhibitors are often used in the clinical pharmacotherapy of COPD.[10–12] They mainly focus on improving symptoms, reducing complications, and regulating lung function, and are mostly used in combination to control symptoms. However, glucocorticoids, β2 agonists, and anticholinergics have obvious side effects.[13–15] Overall, the airway obstruction caused by COPD airway inflammation is barely irreversible, and the current pharmacological treatment to delay disease progress is insufficient to meet the needs of current clinical treatment. Therefore, there is an urgent need to develop safe and effective new drugs for the treatment of COPD.

Epithelial-mesenchymal transition (EMT) is a biological process in which epithelial cells transform into mesenchymal cells that play an important role in the airway remodeling of COPD.[16] Furthermore, airway remodeling is an important regulatory mechanism for airflow limitation in the development of COPD. Recurrent episodes of chronic inflammation lead to airway wall thickening, structural destruction of lung parenchyma, lumen narrowing, increased airflow resistance and emphysema formation, and the process is known as airway remodeling.[17] Studies have shown that airway remodeling in COPD is highlighted by fibrosis of small airways less than 2 mm in diameter, which is associated with abnormal airway epithelial repair and extracellular matrix (ECM) deposition caused by airway inflammation.[18] Repeated airway inflammation stimulates a variety of cells to produce TGF-β1, promotes the transformation of fibroblasts into myofibroblasts, induces epithelial cells to lose epithelial markers and transform into mesenchymal markers, and promotes the EMT process, thereby aggravating airway remodeling and small airway fibrosis.[19] Airway remodeling is an early event in the development of airflow limitation and emphysema in COPD, and EMT is an important pathological basis for airway remodeling and small airway fibrosis in COPD.[20] Therefore, investigating the regulatory mechanism of drugs on the EMT process of COPD is of great significance for the treatment of COPD.

Fritillaria is the dried bulb of various plants of the genus *Fritillaria* in the Liliaceae family, including Bulbus *Fritillariae cirrhosae*, Bulbus *Fritillariae ussuriensis*, Bulbus *Fritillariae pallidiflorae*, Bulbus *Fritillariae thunbergii*, and Bulbus *Fritillariae hupehensis*, etc. There are about 80 species of *Fritillaria* in China, mainly distributed in Sichuan, Xinjiang, Gansu, Hubei, and Anhui.[21] The phytochemical constituents of *Fritillaria* have various pharmacological activities such as antitussive, expectorant, antitumor, anti-inflammatory, antioxidant, protection against lung injury, treatment of bronchitis, etc.[22] Bulbus *Fritillariae pallidiflorae* (BFP), the dried bulbs of *Fritillaria walujewii* Regel or *Fritillaria pallidiflora* Schrenk from the Liliaceae family, which is officially recorded in the Chinese Pharmacopoeia (2020 edition) and widely distributed in the Xinjiang Uygur Autonomous Region.[23] BFP, the Chinese name "Yibeimu", is widely used as a traditional Chinese medicine because of the effect of moistening lungs, eliminating sputum, relieving cough, anti-inflammatory, and antioxidant.[24] BFP contains isosteroid alkaloids, saponins, flavonoids, polysaccharides, coumarins, fatty acid glycerides, amino acids, etc. chemical components, among which alkaloids are the main active ingredients.[25] Previous studies by our research group have shown that the isosteroid alkaloids (verticinone, verticine, imperialine-3-β-D-glucoside, delavine, imperialine, and peimisine) in *Fritillaria* have anti-inflammatory and antioxidant effects.[26,27] Furthermore, imperialine could improve pulmonary function and structural impairment and alleviate the inflammatory response in COPD rat model.[28] However, the effect of the total alkaloid extract from Bulbus *Fritillariae pallidiflorae* (BFP-TA) on COPD has not been reported. Therefore, this study is aimed at investigating the therapeutic effect and molecular mechanisms of BFP-TA in CS-induced COPD mouse model, and providing a reference basis for the rational development and utilization of the medicinal resources of BFP and the development of new drugs for the treatment of COPD.

Materials and Methods

Chemicals and Reagents

Edpetiline (CAS # 32685-93-1), imperialine (CAS # 61825-98-7), peimisine (CAS # 19773-24-1), yibeinoside A (CAS # 98985-24-1), verticinone (CAS # 18059-10-4), delavine (CAS # 98243-57-3), isopeimine (CAS # 23496-43-7), delavinone (CAS # 96997-98-7), and ebeiedinone (CAS # 25650-68-4) were purchased from Chengdu Must Bio-technology (Chengdu, China). The purity of all these substances was above 98%. Jiaozi cigarettes were purchased from Sichuan Zhongyan (Chengdu, China). Dexamethasone (CAS # 50-02-2, Dexa, purity>98%) was purchased from Merck (Darmstadt, Germany). Phosphatase inhibitor (catalog # P1260) and PMSF (catalog # P0100) were purchased from Solaribo Life Sciences (Beijing, China). RIPA buffer (catalog # P0013B), total superoxide dismutase (SOD) detection kit (catalog # S0101S), malondialdehyde (MDA) detection kit (catalog # S0131S), and bicinchoninic acid (BCA) protein kit (catalog # P0010S) were purchased from Beyotime Biotechnology (Shanghai, China). Diethylamine (CAS # 109-89-7), acetonitrile (CAS # 75-05-8), and formic acid (CAS # 64-18-6) used in this experiment were chromatographic grade, and other reagents were analytical grade.

Enzyme-linked immunosorbent assay kits of TNF-α (catalog # JYM0218Mo), IL-6 (catalog # JYM0012Mo), IL-1β (catalog # JYM0531Mo), MMP-9 (catalog # JYM0737Mo), MMP-12 (catalog # JYM0826Mo), and TIMP-1 (catalog # JYM0594Mo) were purchased from Wuhan ColorfulGene Biological Technology (Wuhan, China). The rabbit primary antibodies for GAPDH (catalog # AF7021), MMP-9 (catalog # AF5228), TIMP-1(catalog # AF7007), p38 MAPK (catalog # AF6456), JNK (catalog # AF6318), and Bax (catalog # AF0120) were purchased from Affinity Biosciences (OH, USA). The rabbit primary antibodies for p-p38 MAPK (catalog # 9211), p44/42 (Erk1/2) (catalog # 9102), p-p44/42 (p-Erk1/2) (catalog # 9101), p-JNK (catalog # 4668), and β-actin (catalog # 4967) were purchased from Cell Signaling Technology (Boston, USA). The rabbit primary antibodies for collagen I (catalog # ab260043), E-cadherin (catalog # ab76319), vimentin (catalog # ab92547), and α-SMA (catalog # ab5694), and anti-rabbit HRP-conjugated secondary antibodies (catalog # ab6721) were obtained from Abcam (Cambridge, UK).

Preparation and Material Basis Study of BFP-TA

BFP (purchased from the Gongliu County of Xinjiang Uygur Autonomous Region) are the dried bulbs of *Fritillaria pallidiflora* Schrenk from the Liliaceae family. The plant samples were identified by Professor Bengui Ye of Sichuan University, and the voucher specimens were deposited in the herbarium of the West China School of Pharmacy, Sichuan University. Based on the previous research of our research group,[29,30] BFP-TA was prepared by macroporous adsorbent resin, and the material basis of BFP-TA was analyzed by HPLC-ELSD and UHPLC-MS/MS. The specific methods are described in the Supplementary Material.

Establishment of COPD Mouse Model and Drug Administration

Balb/c mice (SPF, 8 weeks old, male and 18–22g) obtained from Hunan SJA Laboratory Animal Co., Ltd (Changsha, China) were housed in SPF-grade animal facility at 25 °C and 12h-12h of light-dark cycle. Food and water were given as required. The mice were categorized into 6 study groups (20 mice per group): control group, cigarette smoke (CS)-induced COPD group, COPD + dexamethasone (1 mg/kg/d) group, COPD + low-dose (20 mg/kg/d) BFP-TA group, COPD + medium-dose (40 mg/kg/d) BFP-TA group, COPD + high-dose (60 mg/kg/d) BFP-TA group.

The model was established based on a previously reported method.[19] For the CS-induced COPD mouse model, mice were placed in a 70×40 × 25 cm fume box and exposed to 5 filter-tipped cigarettes (tar: 11 mg/cigarette; nicotine: 1.1 mg/cigarette) for 1 h, twice a day, and the interval time between two CS exposures was more than 4 h. CS-induced lasted 6 days per week for 12 weeks. The control group animals were exposed to room air for 12 weeks. At 9–12 weeks, the administration group was administered BFP-TA solution (dissolved in 2% Tween-80) or dexamethasone (dissolved in sterile saline) by a gavage needle 30 minutes before CS exposure. The control group and the CS-induced COPD group were administered 2% Tween-80 by a gavage needle. Each group of mice was weighed and recorded weekly, and the mental status, temperament changes, and general appearance of mice were closely observed throughout the COPD modeling process.

Pulmonary Function Measurement

After 12 weeks of CS exposure, six mice from each group were randomly selected for pulmonary function measurement. The mice were anesthetized by intraperitoneal injection of 1% pentobarbital (60 mg/kg). After 5–7 min, the mice were in a state of deep anesthesia and were in lateral recumbency, the flip response disappeared, the toes or fingers had no response to the stimulus, and they could spontaneously breathe and had a steady respiratory rate. Subsequently, after fixing the mice in a supine position, the neck hair was moistened with alcohol cotton, then the neck skin was cut, a small "T"-shaped opening was cut in the middle of the trachea, and the opening was secured with surgical wires after intubated with a tracheal cannula, the mice were subsequently placed in a computer-connected Buxco pulmonary function system (DSI, NC, USA). The following pulmonary function data were measured: functional residual capacity (FRC), chord compliance (Cchord), forced vital capacity (FVC), forceful expiratory volume in 100 ms (FEV100), peak expiratory flow (PEF), and resistance index (RI). Immediately after pulmonary function measurement, the mice were euthanized by blood collection via cardiac puncture.

Sample Preparation and Histopathology Analysis

After 12 weeks of CS exposure, the rest mice were anesthetized with 1% pentobarbital (60 mg/kg), and the whole blood of mice in each group was collected by cardiac puncture. After centrifugation of the blood (4000 × g, 10 min, 4°C), the supernatant (serum) was stored at −80°C for subsequent cytokine detection. After blood collection, the whole lungs of the mice were quickly removed for photographing and weighing. The lung-body ratio = (lung weight (mg)) / (body weight (g)) ×100%. Subsequently, the left lung tissues were fixed immediately in 4% paraformaldehyde (biosharp, Hefei, China) for 48 h, and the paraffin section (4 μm) was prepared and stained with hematoxylin and eosin (H&E) and Masson's trichrome staining for subsequent histopathological analysis. Then the right lung tissues from each group of mice were removed and stored at −80°C for Western blot analysis.

Histopathological Score

To investigate the effect of BFP-TA on the lung tissue of COPD mice more directly, this research constructs the scoring standard based on the results of H&E staining. The H&E staining score contains three classification evaluation indexes: emphysema, inflammatory cell infiltration, and airway structural damage. Each classification contains four levels (none, mild, moderate, and serious), and the scoring standards are shown in Table 1. Three randomly selected fields of each sample were photographed and scored at 100× magnification, the mean score represented the pathological level of the selected sample, and the H&E staining score result showed the average histopathological scores of each group of lung tissue samples. In the same way, based on the results of Masson staining, three randomly selected fields of each sample were photographed at 100× magnification, then the percentage of collagen fibers in lung tissue was statistically analyzed using ImageJ software, and the ratio of "collagen fiber deposition area/pathology section area" under the view field was used as a criterion for evaluating the degree of collagen deposition.

Determination of TNF-α, IL-1β, IL-6, MMP-9, MMP-12, TIMP-1, SOD and MDA Levels

The levels of TNF-α, IL-1β, IL-6, MMP-9, MMP-12, and TIMP-1 in the serum of mice were subsequently determined using ELISA kits based on the manufacturer's instructions. Absorbance values were measured at 450 nm using

Table 1 The H&E Staining Score Standards

Degree of Change	Emphysema	Inflammatory Cell Infiltration	Airway Structural Damage
None	0	0	0
Mild	1	1	1
Moderate	2	2	2
Serious	3	3	3

a microplate reader (BioRad, VA, USA). The levels of MDA and SOD in the serum of mice were determined using the SOD detection kit and the MDA detection kit based on the manufacturer's instructions.

Western Blot

Total proteins from lung tissue were extracted using RIPA lysis buffer (RIPA: PMSF: phosphatase inhibitor = 100:1:1), and the protein concentrations in each group were quantified with the BCA protein assay kit. After loading with sample loading buffer, the protein samples were heated at 100°C for 10 min. Equal amounts of proteins were separated by sodium dodecyl sulfate-polyacrylamide gel electrophoresis (SDS-PAGE) and transferred to polyvinylidene fluoride membranes (Millipore, MA, USA). Subsequently, the membrane was blocked with 5% skim milk for 1 h at room temperature and incubated with specific primary antibodies (1:1000) at 4°C overnight. After washed three times with TBST, the membrane was incubated with anti-rabbit HRP-conjugated secondary antibodies (1:10,000) for 1 h at room temperature. Afterward, the membrane was washed with TBST, and protein bands were detected on the GelView 5000Plus Gel Imaging System (Biolight, Guangzhou, China) using the BeyoECL Plus (Millipore, MA, USA) and analyzed with ImageJ software.

Statistical Analysis

The data was expressed as mean ± SD, multiple comparisons were performed using One-way ANOVA followed by the Bonferroni posttest. All analyses were performed using GraphPad Prism 8 (San Diego, CA, USA). The value of $P < 0.05$ was considered statistically significant.

Results

The Content of Total Alkaloid in BFP-TA

The linear relationship between alkaloid concentration and OD415 can be expressed as:

$$Y = 0.9708X - 0.0004 \left(R^2 = 0.9994\right)$$

According to the calibration equation, the total alkaloid content in BFP-TA is 64.28%.

The HPLC-ELSD and UHPLC-MS/MS Analysis of BFP-TA

Based on comparing the retention time of each compound with the standard compounds by HPLC-ELSD, eight isosteroid alkaloids were identified in the BFP-TA, namely edpetiline, imperialine, peimisine, yibeinoside A, verticinone, isopeimine, delavinone, and ebeiedinone. The HPLC diagram of BFP-TA is shown in Figure 1A.

UHPLC-MS/MS analysis of the BFP-TA was carried out in positive ionization modes, and the content of nine isosteroid alkaloids in BFP-TA was calculated using the calibration equation. As shown in Table 2, the content of imperialine (34.68%) is the highest, followed by edpetiline (13.29%), and the total content of nine alkaloids is 60.76% in BFP-TA. The total ion chromatogram of nine alkaloids in a mixed standard solution is shown in Figure 1B, and the chemical structures of the nine alkaloids are shown in Figure 1C.

Animal General Appearance and Weight Changes

The flow of the animal experiment is shown in Figure 2A. In the course of animal experiments, the control group mice had no deaths, glossy fur, uniform respiration, and normal activities. However, the COPD model group mice had lusterless and yellowish fur, partly fur loss, restlessness, piled up when smoking, tiredness, huddle, sweatiness, shortness of breath, and drinking and urinating a lot. As shown in Figure 2B, the body weight changes within 8–12 weeks after administration were compared, and the results showed that the weight growth of mice in each administration group was accelerated compared with the COPD model group. Furthermore, the body weight of mice in the COPD model group was significantly decreased compared with the control group at week 12 ($P < 0.0001$) (Figure 2C). After treated with different doses of BFP-TA, the body weight of mice all significantly increased compared with the COPD model group ($P < 0.0001$), among which the high-dose BFP-TA group showed the best effect. These results suggest that BFP-TA could reverse the trend of CS-induced body weight loss in mice.

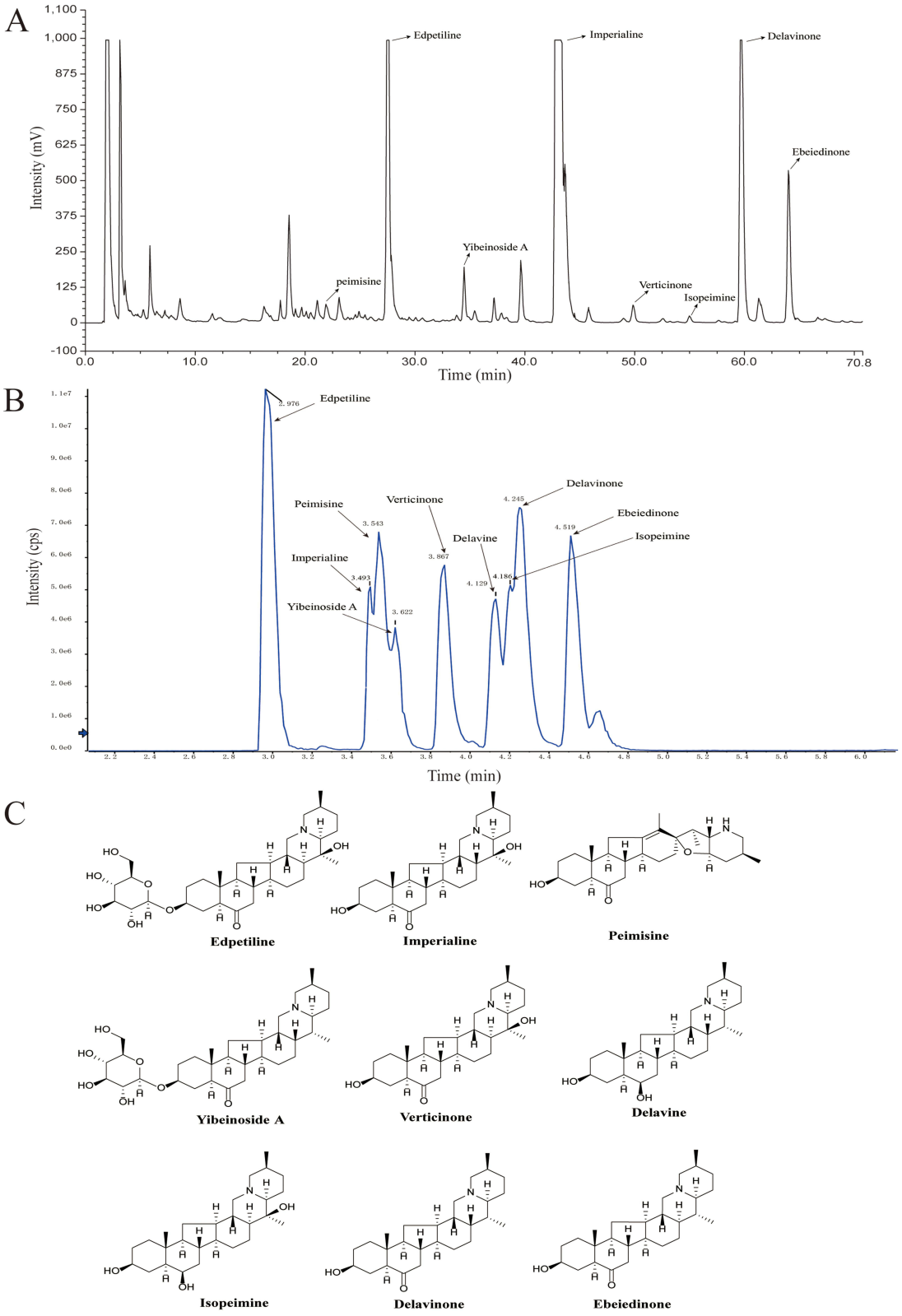

Figure 1 HPLC-ELSD and UHPLC-MS/MS analyses of BFP-TA. (**A**) HPLC diagram of BFP-TA. (**B**) The total ion chromatogram of nine alkaloids in a mixed standard solution was determined by UHPLC-MS/MS. (**C**) Chemical structures of nine alkaloids.

Table 2 The UHPLC-MS/MS Analysis of BFP-TA

Identification Compound	Retention Time (Min)	Content	Q1 Mass (Da)	Q3 Mass (Da)	Molecular Weight	Formula
Edpetiline	2.976	13.29%	592.4	574.4	591.78	$C_{33}H_{53}NO_8$
Imperialine	3.493	34.68%	430.4	138.1	429.64	$C_{27}H_{43}NO_3$
Peimisine	3.543	0.22%	428.3	114.1	427.62	$C_{27}H_{41}NO_3$
Yibeinoside A	3.622	1.18%	576.4	414.4	575.78	$C_{33}H_{53}NO_7$
Verticinone	3.867	0.80%	430.3	148.2	429.64	$C_{27}H_{43}NO_3$
Delavine	4.129	0.15%	416.4	98.1	415.65	$C_{27}H_{45}NO_2$
Isopeimine	4.186	0.24%	432.4	414.4	431.65	$C_{27}H_{45}NO_3$
Delavinone	4.245	6.92%	414.4	98.1	413.64	$C_{27}H_{43}NO_2$
Ebeiedinone	4.519	3.28%	414.4	91.1	413.64	$C_{27}H_{43}NO_2$

BFP-TA Ameliorates Lung Morphology in the COPD Mouse Model

As shown in Figure 2D, the lung morphology of mice in each group was observed, and the results showed that the surface of lung tissues in the control group was smooth and flat, with light pink color. However, the surface of lung tissues in the COPD model group was rough and gray, with some gray-black patches. After treated with dexamethasone and different doses of BFP-TA, the general appearance of the lung tissue was improved. As shown in Figure 2E, the lung-body ratio of the mice in the COPD model group was significantly increased compared with the control group ($P < 0.001$), and this trend was significantly suppressed in the medium and high-dose BFP-TA groups ($P < 0.05$). These results suggest that BFP-TA could ameliorate CS-induced morphological changes in mouse lung tissue and inhibit the elevation of lung-body ratio.

BFP-TA Ameliorates Pulmonary Function in the COPD Mouse Model

Pulmonary function is the key standard for COPD diagnosis and treatment. As shown in Figure 3A–E, compared with the control group, FRC, Cchord and RI were significantly increased in the COPD model groups ($P < 0.05$, $P < 0.001$, $P < 0.001$), while FEV100/FVC and PEF were significantly decreased ($P < 0.001$, $P < 0.01$). These data further confirmed the reliability of the COPD model. After treated with dexamethasone, FRC and Cchord were significantly decreased ($P < 0.05$, $P < 0.01$), while FEV100/FVC was significantly increased ($P < 0.001$). Compared with the model group, all different doses of BFP-TA groups tended to ameliorate the above indexes in a dose-dependent manner. Overall, the improvement of CS-induced pulmonary function decline in the high-dose BFP-TA group was better than the dexamethasone group.

BFP-TA Alleviates Lung Histopathology in the COPD Mouse Model

H&E staining was used to assess the effect of BFP-TA on the lung histopathology of mice. As shown in Figure 4A, in the control group, the bronchial mucosal epithelium of the lung tissue was intact, the cilia were neatly arranged, there was no inflammatory cell infiltration around the bronchial tubes and the blood vessels, and the alveolar intervals did not show obvious fracture or fusion. Based on the results of the H&E staining score (Figure 4B), compared with the control group, the lung tissue of the COPD model group showed bronchial wall thickening, obvious lung tissue structure damage, bronchial mucosa epithelial detachment, and largely inflammatory cells infiltration in the lung interstitial, alveolar obvious expansion, part of the alveolar septum fracture, alveoli irregularly enlarged and fusion ($P < 0.0001$). After treated with BFP-TA, the lung tissue structure was significantly improved and repaired ($P < 0.0001$), alveolar dilatation and rupture were reduced, and the bronchial wall was thinned. However, some inflammatory cell infiltration was still visible in the lung tissue of the dexamethasone group and the low-dose BFP-TA group, which was obviously alleviated in the medium-dose and high-dose BFP-TA groups. These results suggest that BFP-TA could alleviate lung histopathology damage in COPD mice.

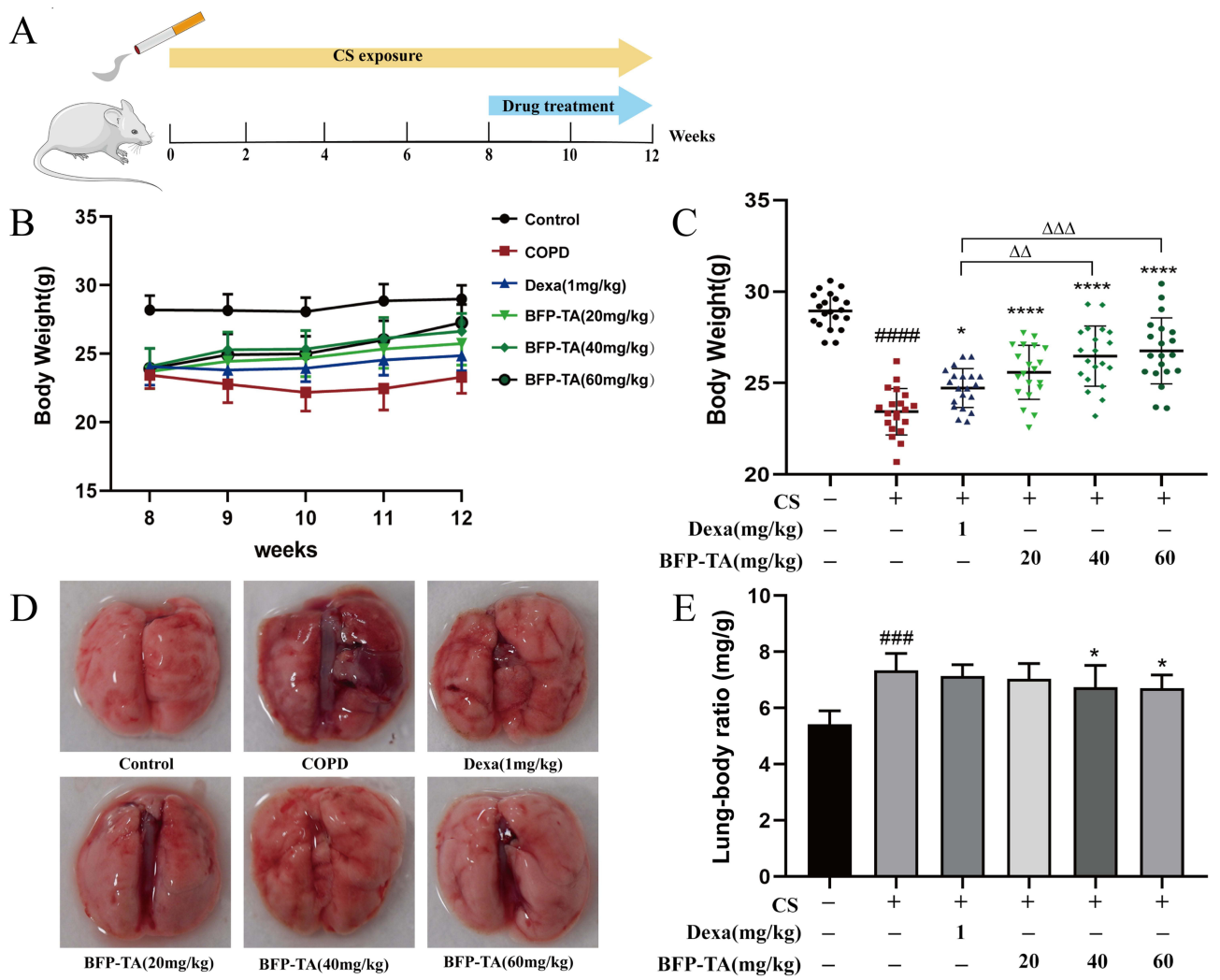

Figure 2 Effect of BFP-TA on the general appearance, weight, and lung morphological changes in the COPD mouse model. (**A**) Method of mice experiments. (**B**) The body weight changes of each group of mice within 8–12 weeks. (**C**) Body weight of mice in each group at week 12. (**D**) Representative images of the lung morphology of mice in each group. (**E**) The lung-body ratio of mice in each group. Data were presented as mean ± SD (n=20), $^{\#\#\#}P < 0.001$, $^{\#\#\#\#}P < 0.0001$ compared to the control group; $^{*}P < 0.05$, $^{****}P < 0.0001$ compared to the COPD model group; $^{\Delta\Delta}P < 0.01$, $^{\Delta\Delta\Delta}P < 0.001$ compared to the Dexa group.

Masson's trichrome staining was used to assess the effect of BFP-TA on the collagen deposition in the lung tissue of mice (Figure 4C). The collagen fibers appeared to be dark blue after Masson's trichrome staining, which was mainly distributed in the peribronchiolar, perivascular, and interalveolar. As shown in Figure 4D, the expression of collagen fibers was significantly elevated in the lung tissues of the COPD group ($P < 0.0001$). After treated with different doses of BFP-TA, the collagen fiber volume fraction in lung tissue was significantly reduced ($P < 0.0001$), among which the high-dose BFP-TA showed a better effect than the dexamethasone group ($P < 0.05$). These results suggest that BFP-TA could reduce the deposition of collagen fibers in the lung tissue of COPD mice.

BFP-TA Alleviates the Levels of Pro-Inflammatory Cytokine in the COPD Mouse Model

To evaluate the effect of BFP-TA on the inflammatory response in CS-induced COPD mice, the levels of pro-inflammatory cytokine (TNF-α, IL-1β, and IL-6) in mouse serum were measured by ELISA kits. As shown in Figure 5A–C, the levels of TNF-α, IL-1β, and IL-6 were significantly increased in the COPD model group ($P < 0.001$, $P < 0.0001$, $P < 0.0001$), suggesting that the organism was damaged by inflammatory response. However, the

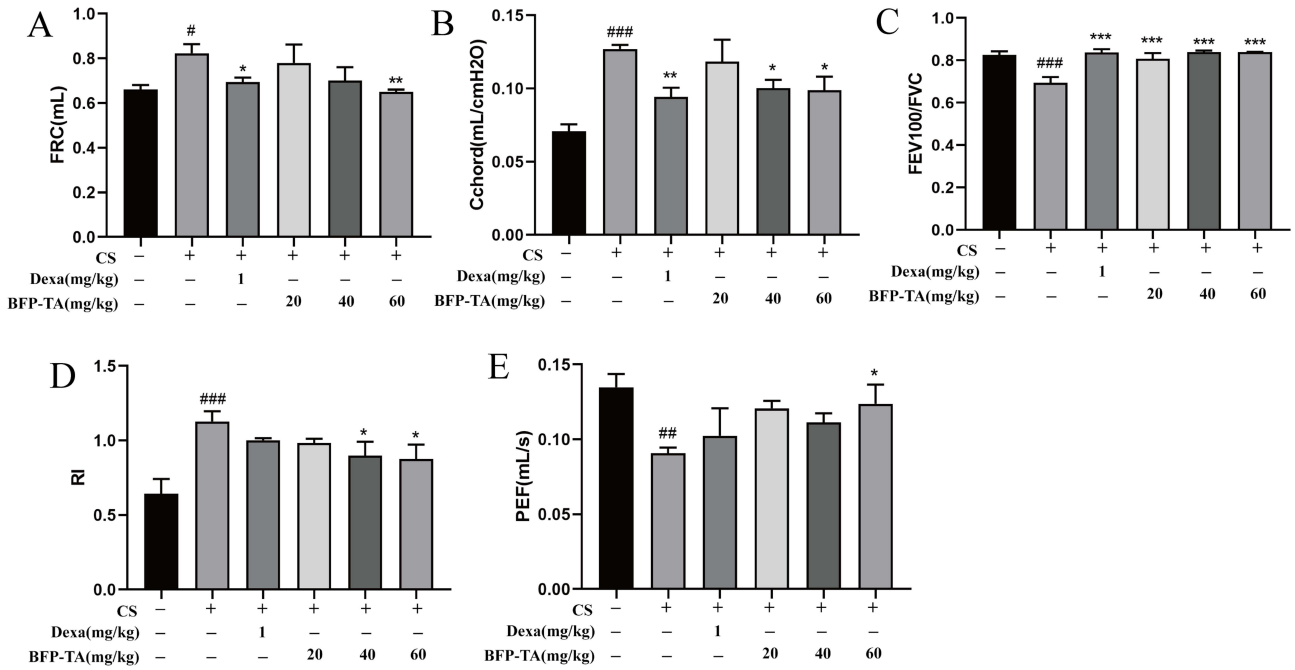

Figure 3 Effect of BFP-TA on pulmonary function in the COPD mouse model. (**A**–**E**) FRC, Cchord, FEV100/FVC, RI, and PEF in each group of mice were determined by pulmonary function measurement. Data were presented as mean ± SD (n=6), $^{\#}P < 0.05$, $^{\#\#}P < 0.01$, $^{\#\#\#}P < 0.001$ compared to the control group; $^{*}P < 0.05$, $^{**}P < 0.01$, $^{***}P < 0.001$ compared to the COPD model group.

levels of pro-inflammatory cytokines were decreased in all administration groups in a dose-dependent manner, among which the effect of high-dose BFP-TA was superior to the dexamethasone group. These results suggest that BFP-TA could attenuate the inflammatory response by inhibiting the expression of pro-inflammatory factors in CS-induced COPD mice.

BFP-TA Regulates the Levels of Matrix Metalloproteinase in the COPD Mouse Model

Matrix metalloproteinases (MMPs) and matrix metalloproteinase inhibitors (TIMPs) are important systems that regulate ECM synthesis and degradation, which play an important role in the emphysema of COPD. As shown in Figure 5D–F, the levels of MMP-9 and MMP-12 were significantly increased in the COPD model group ($P < 0.001$, $P < 0.0001$), which were decreased in the BFP-TA group in a dose-dependent manner, and the high-dose BFP-TA group showed a better effect than the dexamethasone group. Furthermore, the level of TIMP-1 was significantly decreased in the COPD model group ($P < 0.0001$), which was significantly reversed by the administration of dexamethasone, medium-dose and high-dose BFP-TA ($P < 0.01$, $P < 0.001$, $P < 0.05$). These results suggest that BFP-TA could regulate protease/antiprotease homeostasis by modulating the disorder of MMPs/TIMPs homeostasis in CS-induced COPD mice.

BFP-TA Regulates the Levels of Oxidative Stress Markers in the COPD Mouse Model

The effects of BFP-TA on oxidative damage in CS-induced COPD mice were investigated by determining the levels of MDA and SOD. As shown in Figure 5G and H, the level of MAD was significantly increased while the level of SOD was significantly decreased in the serum of CS-induced COPD mice ($P < 0.001$, $P < 0.01$). BFP-TA administration significantly inhibited the increase of MDA levels in a dose-dependent manner ($P < 0.001$), among which the effect of the high-dose BFP-TA was superior to the dexamethasone group. Furthermore, medium- and high-dose BFP-TA administration significantly reversed the SOD levels ($P < 0.05$, $P < 0.01$). These results suggest that BFP-TA could attenuate CS-induced oxidative damage by regulating the levels of oxidative stress markers in COPD mice.

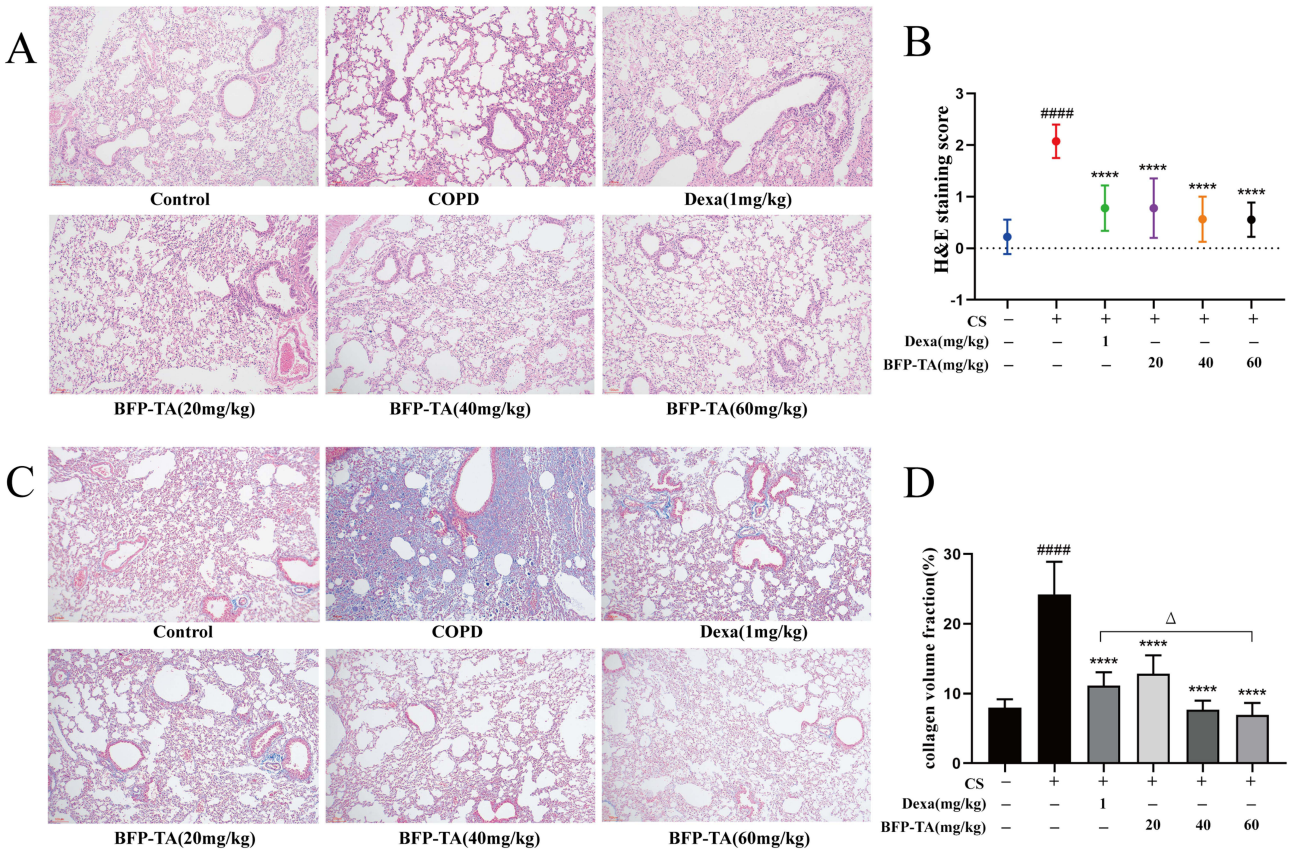

Figure 4 Effect of BFP-TA on lung histopathology in the COPD mouse model. (**A**) Representative images of H&E staining in each group of mice (100×). (**B**) H&E staining score in each group of mice. (**C**) Representative images of Masson's trichrome staining in each group of mice (100×). (**D**) Collagen fibers volume fraction in each group of mice. Data were presented as mean ± SD (n=6), $^{\#\#\#\#}$P < 0.0001 compared to the control group; ****P < 0.0001 compared to the COPD model group; $^{\Delta}$P < 0.05 compared to the Dexa group.

Effect of BFP-TA on the Regulation of EMT in the COPD Mouse Model

Airway remodeling is the main pathological feature of COPD, and EMT is a key factor in airway remodeling. Therefore, the expression of EMT-associated proteins in CS-induced mouse lung tissues was evaluated by Western blot. As shown in Figure 6A–H, the Western blot results showed that the levels of Collagen I, Vimentin, α-SMA, MMP-9, MMP-9/TIMP-1, and Bax in the COPD model group were significantly increased ($P < 0.001$, $P < 0.05$, $P < 0.05$, $P < 0.0001$, $P < 0.001$, $P < 0.0001$), while the level of E-cadherin was significantly decreased ($P < 0.0001$). After treated with certain doses of BFP-TA, the levels of Collagen I, Vimentin, α-SMA, MMP-9, MMP-9/TIMP-1, and Bax were decreased, while the level of E-cadherin was increased. Furthermore, the dexamethasone group also had a regulatory effect on CS-induced changes in the levels of EMT-related proteins, except for E-cadherin. These results suggest that BFP-TA may play a protective role against COPD by inhibiting CS-induced EMT in mouse lung tissue, and the effects were similar to the positive drug dexamethasone.

Effect of BFP-TA on the Regulation of MAPK Signaling Pathway in the COPD Mouse Model

Airway inflammation is one of the main features of COPD, which is manifested by the infiltration of inflammatory cells and the release of inflammatory factors. The mitogen-activated protein kinase (MAPK) signaling pathway is now widely recognized as an important pathway that regulates inflammatory signals. As shown in Figure 7A–D, the Western blot results showed that the levels of p-JNK/JNK, p-P38/P38, and p-ERK/ERK in the COPD model group were significantly increased ($P < 0.0001$, $P < 0.001$, $P < 0.0001$). After treated with dexamethasone, the expressions of p-JNK/JNK, p-P38/P38, and p-ERK/ERK were significantly decreased ($P < 0.01$, $P < 0.05$, $P < 0.01$). Moreover, the levels of p-JNK/JNK, p-P38/P38, and p-ERK/ERK were decreased in certain doses of BFP-TA groups, among which the inhibitory effect on

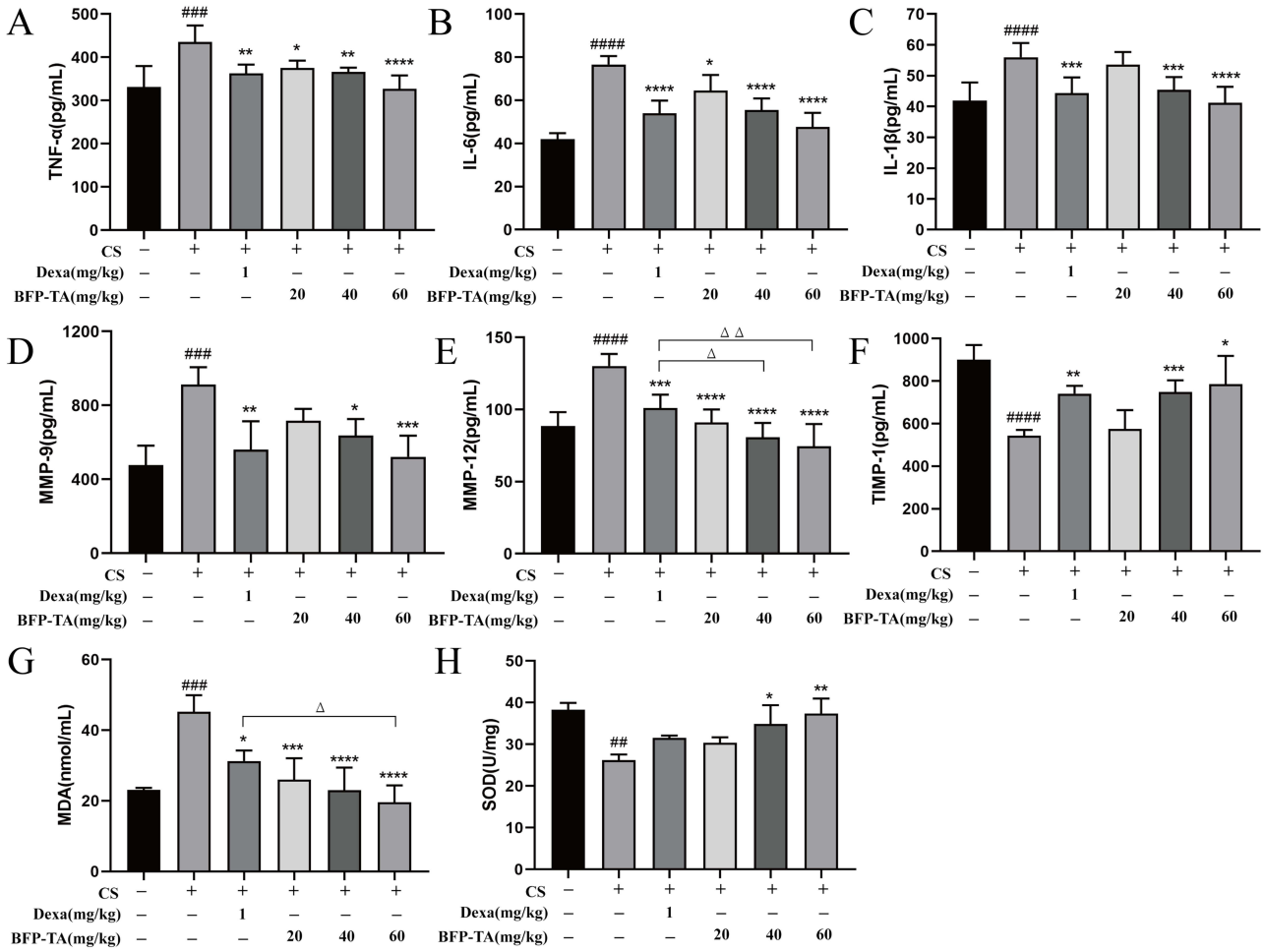

Figure 5 Effect of BFP-TA on pro-inflammatory cytokines, MMPs, and oxidative stress cytokines in the COPD mouse model. (**A**–**C**) The levels of TNF-α, IL-6, and IL-1β in the serum of each group of mice. (**D**–**F**) The levels of MMP-9, MMP-12, and TIMP-1 in the serum of each group of mice. (**G**–**H**) The levels of MDA and SOD in the serum of each group of mice. Data were presented as mean ± SD (n=6), $^{\#\#}P < 0.01$, $^{\#\#\#}P < 0.001$, $^{\#\#\#\#}P < 0.0001$ compared to the control group; $^{*}P < 0.05$, $^{**}P < 0.01$, $^{***}P < 0.001$, $^{****}P < 0.0001$ compared to the COPD model group; $^{\Delta}P < 0.05$, $^{\Delta\Delta}P < 0.01$ compared to the Dexa group.

p-ERK/ERK in the high-dose BFP-TA group was superior to the dexamethasone group ($P < 0.01$). These results suggest that BFP-TA potentially inhibits the activation of the MAPK signaling pathway, thereby attenuating CS-induced inflammatory responses.

Discussion

This study aimed to investigate the therapeutic effect and molecular mechanisms of BFP-TA in CS-induced COPD mouse model. As is well known, smoking is the leading risk factor for COPD,[31] and the oxidant in CS contains large amounts of free radicals and ROS that cause direct damage to the airway epithelial cells.[32] Furthermore, the COPD animal model is the primary method for studying drug efficacy and disease pathogenesis. In this study, a 12-week CS exposure was used to establish the COPD mouse model based on previous reports with appropriately adjusted,[19,33,34] then BFP-TA was administered by gavage at weeks 9–12 of CS exposure. Corticosteroids are a first-line therapeutic strategy against COPD airway inflammation.[35] Therefore, the potent anti-inflammatory drugs of the corticosteroid class (dexamethasone) were used as positive control in this study.[36] Subsequently, the animal experiment results showed that BFP-TA could attenuate CS-induced weight loss and improve lung tissue morphology in COPD mice. The histopathological examination showed that BFP-TA could reduce alveolar dilatation and rupture, inflammatory cell infiltration, degree of emphysema, degree of airway thickening, and collagen deposition in CS-induced COPD mouse model, thereby

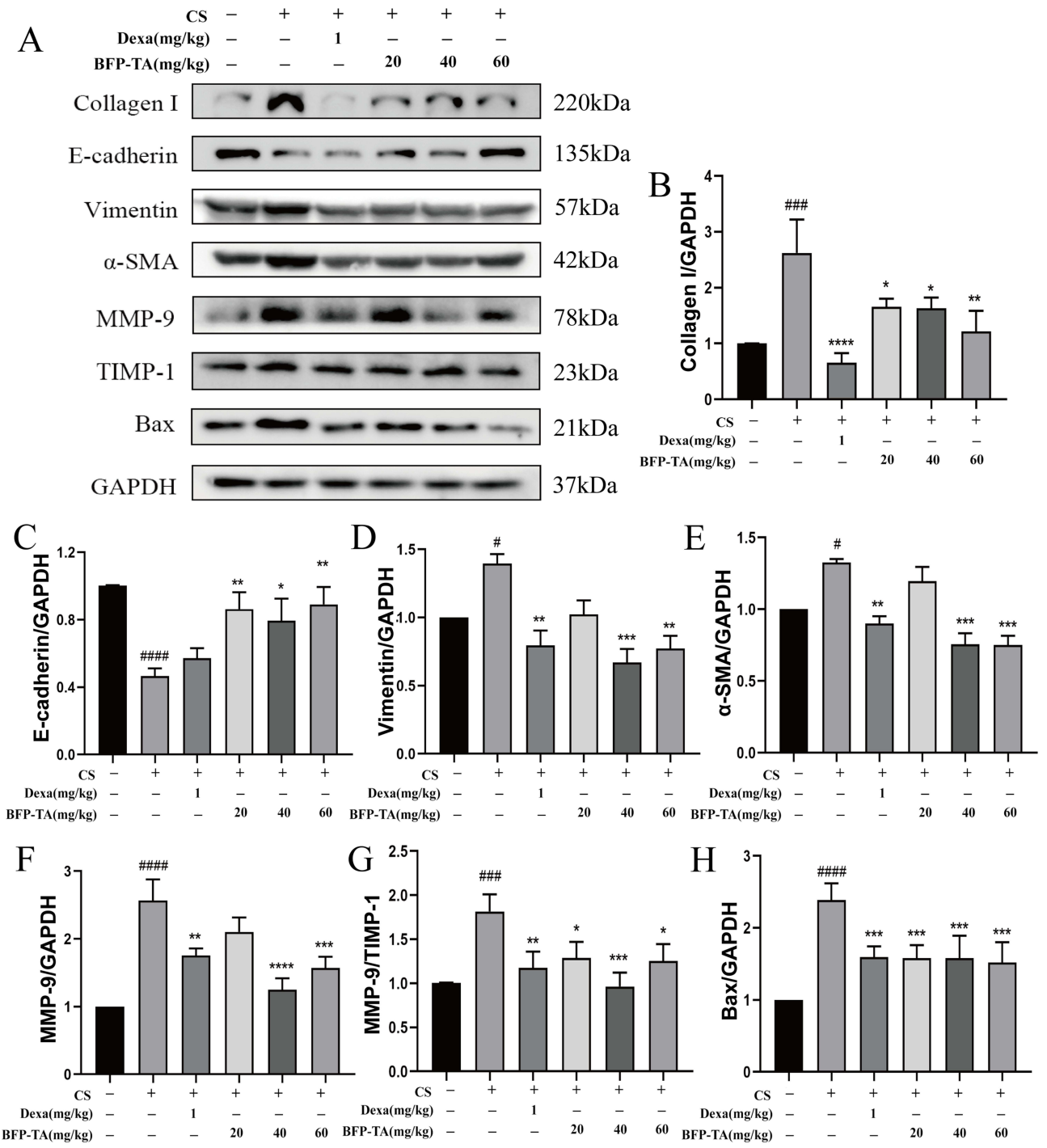

Figure 6 Effect of BFP-TA on the expression of EMT-related proteins in the COPD mouse model. (**A**–**H**) The relative expression levels of Collagen I, E-cadherin, Vimentin, α-SMA, MMP-9, TIMP-1, and Bax were determined by Western blot. Data were presented as mean ± SD (n =3), $^{\#}$P < 0.05, $^{\#\#\#}$P < 0.001, $^{\#\#\#\#}$P < 0.0001 compared to the control group; *P < 0.05, **P < 0.01, ***P < 0.001, ****P < 0.0001 compared to the COPD model group.

improving and repairing lung tissue structure. Furthermore, the COPD mice had thickened and narrowed airways in the lung tissue, increased collagen secretion, ECM deposition and fibrosis of the small airways, leading to an elevated lung-body ratio,[37] which was inhibited by high- and medium-doses BFP-TA. Pulmonary function is considered the most important adjunctive test for the diagnosis of COPD because it shows small airway pathology and is more sensitive than morphological changes in the lungs.[38] The results of this study showed that CS-induced COPD model mice exhibited significant airflow restriction and pulmonary hyperinflation, such as decreased FEV100/FVC and PEF values and

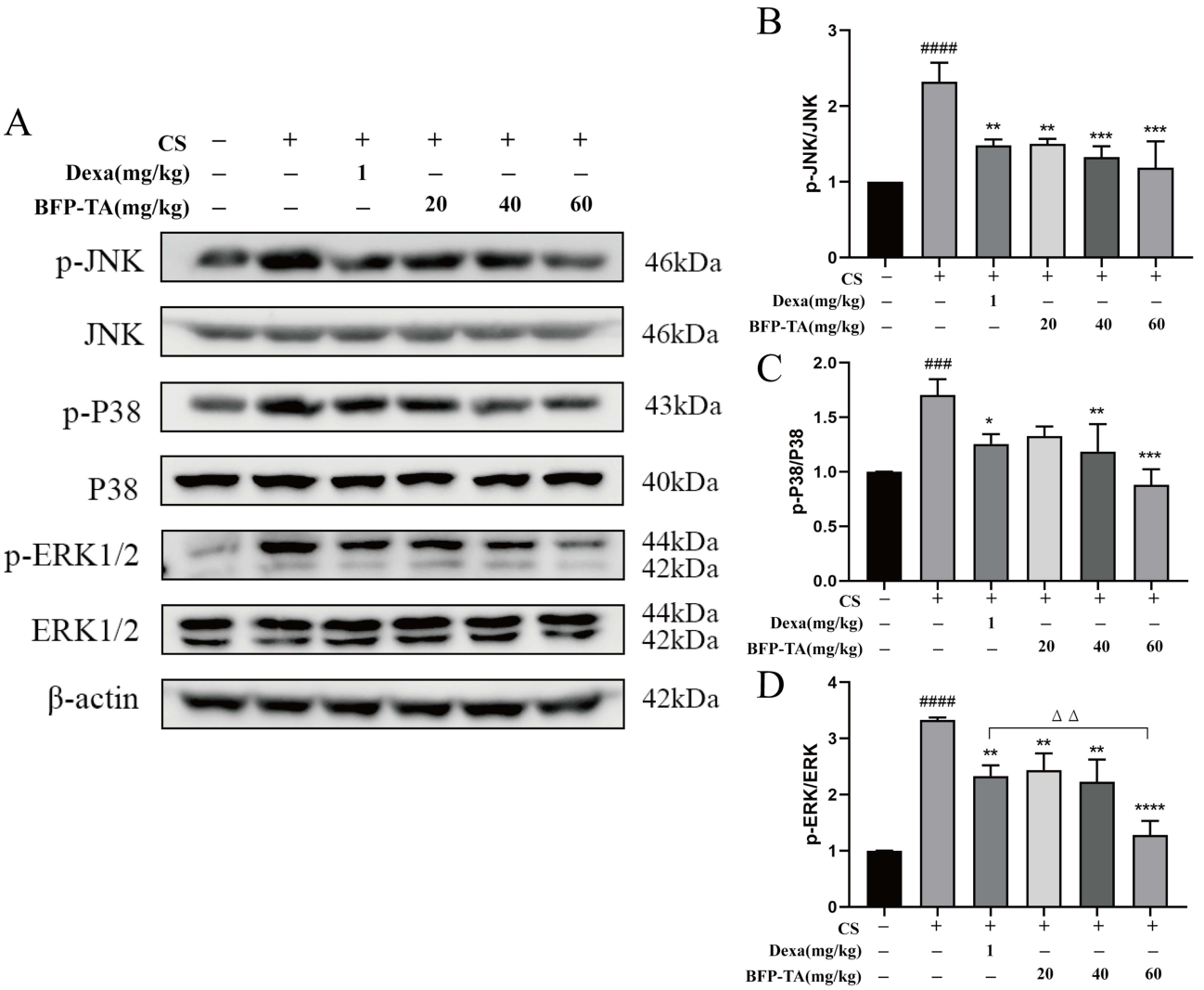

Figure 7 Effect of BFP-TA on the expression of MAPK signaling pathway-related proteins in the COPD mouse model. (**A**–**D**) The relative expression levels of p-JNK, JNK, p-P38, P38, p-ERK1/2, and ERK1/2 were determined by Western blot. Data were presented as mean ± SD (n =3), $^{\#\#\#\#}P < 0.001$, $^{\#\#\#\#\#}P < 0.0001$ compared to the control group; $^{*}P < 0.05$, $^{**}P < 0.01$, $^{***}P < 0.001$, $^{****}P < 0.0001$ compared to the COPD model group; $^{\Delta\Delta}P < 0.01$ compared to the Dexa group.

increased FRC, Cchord, and RI values. These data further demonstrate the reliability of the model. After treated with BFP-TA, the values of FRC, Cchord, and RI were decreased while FEV100/FVC and PEF were increased in CS-induced COPD model mice, indicating that the intervention of BFP-TA could reverse the decreasing trend of pulmonary function, improve airflow restriction, and attenuate emphysema in CS-induced COPD mouse model.

Subsequently, the levels of pro-inflammatory cytokines, MMPs, and oxidative stress markers in the serum of mice were determined. Airway epithelial cells are an important barrier for defense against airborne irritants and pathogens. When the body is stimulated by CS, airway epithelial cells will overproduce pro-inflammatory cytokines (eg, TNF-α, IL-6, and IL-1β) that recruit a variety of inflammatory cells, thereby triggering airway inflammation.[39] Furthermore, MMP-9 and MMP-12 are the main MMPs in lung tissue. Under conditions of inflammation and oxidative stress, bronchial epithelial cells, alveolar epithelial cells and endothelial cells in the lungs can produce largely MMP-9 and MMP-12, which can degrade the ECM, aggravate the inflammatory reaction in the lungs by converging inflammatory cells, and destroy the lung tissue structure.[40] TIMP-1 can inhibit the zymogen activation of MMPs and inhibit their activity, which plays an important role in regulating the balance of ECM degradation. Meanwhile, smoking-induced oxidative stress is also an important factor in the development of COPD.[41] When the body is stimulated by smoke, ROS will be produced in large quantities and damage the antioxidant defense system, thus causing damage to the lung tissue. MDA is the product

of lipid peroxidation, which can indirectly show the degree of ROS attack. SOD is a part of the antioxidant enzyme system that can scavenge the oxygen free radicals in the body.[42] Consistent with prior studies, our studies indicated that CS induces could increase the levels of proinflammatory cytokines, MMPs and MDA, and decrease the levels of TIMP-1 and SOD in the serum of COPD model mice, which was significantly reversed by BFP-TA administration. These results suggest that BFP-TA may exert anti-inflammatory effect by inhibiting the production of pro-inflammatory cytokines; increasing the level of TIMP-1 to inhibit the activity of MMPs, thereby attenuating CS-induced emphysema; and regulating the level of oxidative stress cytokines to attenuate CS-induced oxidative damage.

Subsequently, the related protein expressions of the EMT and MAPK signaling pathways in the lung tissues of mice were detected by Western blot. EMT is considered an important signaling process in the pathogenesis of COPD.[43] Therefore, investigating the effect of BFP-TA on the EMT process is important for elucidating the molecular mechanism by which BFP-TA attenuates airway remodeling and emphysema in COPD mice. It is well known that CS can activate the EMT process through multiple mechanisms, leading to pro-inflammatory cytokine release and loss of epithelial cell integrity.[44] During the EMT process, airway epithelial cells turn into mesenchymal cells after the loss of tight junctions, and the expression of epithelial markers such as cell adhesion molecules (eg, E-cadherin) is reduced, and the production of ECM (eg, collagen I) is excessive.[45] Meanwhile, the cytoskeleton dominated by CK18 is transformed into a cytoskeleton dominated by vimentin and α-SMA.[19] Furthermore, repeated airway inflammation stimulates a variety of cells to produce TGF-β1, which promotes fibroblast-to-myofibroblast transformation,[46] inducing increased α-SMA level and collagen secretion, and an imbalance in the ratio of MMPs/TIMPs. Studies have shown that MMPs/TIMPs play a key role in maintaining the protease/antiprotease balance.[47] Excessive protease/antiprotease imbalance will lead to ECM destruction, indirectly acting on alveolar cells, and alveolar cell apoptosis will further promote ECM destruction. Furthermore, the apoptotic response resulting from sustained cellular injury is also a key factor in the pathogenesis of COPD.[48] Consistent with prior studies, our studies indicated that CS induces could decrease the level of epithelial markers (E-cadherin), and increase the levels of mesenchymal markers (vimentin, α-SMA), collagen I, MMP-9, MMP-9/TIMP-1 and Bax, suggesting that CS activated the EMT process and induced protease/antiprotease imbalance. After treated with BFP-TA, the above trends were significantly reversed, suggesting that BFP-TA could inhabit the CS-induced EMT process. These results showed that BFP-TA may protect lung tissues from CS-induced airway remodeling and emphysema by regulating the EMT process.

As is well known, COPD is a common chronic inflammatory airway disease, and the MAPK signaling pathway plays a key role in regulating COPD-related phenotypes, including inflammation and emphysema.[49,50] Therefore, investigating the regulatory mechanism of BFP-TA on the MAPK signaling pathway in CS-induced COPD mice is of great significance for elucidating the anti-inflammatory effect of BFP-TA. Many studies have shown that cigarette smoke induces activation of the MAPK signaling pathway with increased levels of phosphorylated ERK1/2, JNK, and p38 MAPK,[51–53] which is consistent with this study. After treated with BFP-TA, the expression of phosphorylated ERK1/2, JNK, and p38 MAPK were significantly inhibited. Therefore, these results suggest that the protective effect of BFP-TA on CS-induced inflammation and alveolar epithelial cell injury is potentially related to the inhibition of MAPK signaling pathway. Although some important discoveries are revealed by this study, there are also some limitations. First, the specific active components of BFP-TA that delay the disease process of CS-induced COPD still need further investigation. Second, the specific molecular mechanism and signal transduction process by which BFP-TA attenuates the inflammatory response by the MAPK signaling pathway in CS-induced COPD mice still needs further investigation. In our next work, we will further analyze the specific active components in BFP-TA that exert anti-COPD effect through pharmacokinetics, serum pharmacology, and serum medicinal chemistry. Furthermore, we will explore the molecular mechanism by which BFP-TA attenuates the inflammatory response in COPD by further analyzing the regulatory effect of BFP-TA on key signaling molecules in the MAPK signaling pathway. Overall, in terms of practical significance, this study provides data support to first demonstrate that BFP-TA can delay the disease process of CS-induced COPD and preliminary reveal that the molecular mechanism is related to alleviating airway remodeling and inflammation. In terms of application prospects, this study is of reference value for the development of innovative drugs for the treatment of COPD.

Conclusion

To our knowledge, this study is the first to demonstrate the protective effect and potential therapeutic mechanism of BFP-TA on CS-induced COPD mouse model. The results showed that BFP-TA could delay the progression of COPD by inhibiting CS-induced weight loss, reducing the overproduction of pro-inflammatory factors and MMPs, modulating oxidative stress cytokines, attenuating inflammatory cell infiltration and emphysema, decreasing the deposition of collagen fibers, and improving pulmonary function in CS-induced COPD mice. Further studies preliminary demonstrate that BFP-TA may attenuate CS-induced airway remodeling by inhibiting the EMT process, which was evidenced by the changes in specific markers and phenotypic. Furthermore, BFP-TA potentially attenuates CS-induced inflammatory response by inhibiting the activation of the MAPK signaling pathway, which was evidenced by the inhibition of phosphorylation levels in subfamilies. However, the specific active components and molecular mechanism of BFP-TA in anti-COPD still need further investigation, and we will consider these questions seriously in our next work. Overall, this study will provide data support for elucidating the protective effect and molecular mechanism of BFP-TA on the CS-induced COPD model and developing new drugs for the treatment of COPD.

Abbreviations

COPD, chronic obstructive pulmonary disease; BFP, Bulbus *Fritillariae pallidiflorae*; BFP-TA, the total alkaloid extract from Bulbus *Fritillariae pallidiflorae*; Dexa, dexamethasone; SOD, superoxide dismutase; MDA, malondialdehyde; CS, cigarette smoke; FRC, functional residual capacity; Cchord, chord compliance; FVC, forced vital capacity; FEV100, forceful expiratory volume in 100 ms; PEF, peak expiratory flow; RI, resistance index; H&E, hematoxylin & eosin; SDS-PAGE, sulfate-polyacrylamide gel electrophoresis; MMPs, matrix metalloproteinases; EMT, epithelial-mesenchymal transition.

Data Sharing Statement

The data that support the findings of this study are available from the corresponding author upon reasonable request. We have permission to collect the plant samples under study. The study methods comply with Chinese guidelines.

Ethics Statement

All animal experiments were approved by the Ethics Committee of Sichuan University (license number: SCXK (Xiang) 2019-0004), and experimental animals received welfare in accordance with the National Institutes of Health guidelines.

Author Contributions

All authors made a significant contribution to the work reported, whether that is in the conception, study design, execution, acquisition of data, analysis and interpretation, or in all these areas; took part in drafting, revising or critically reviewing the article; gave final approval of the version to be published; have agreed on the journal to which the article has been submitted; and agree to be accountable for all aspects of the work.

Funding

This research was supported by the major science and technology research project in 2021 from Tibet Science and Technology Department (NO. XZ202101ZD0021G), the science and technology major project of Tibetan Autonomous Region of China (NO. XZ202201ZD0001G01, NO. XZ202201ZD0001G06), the Funds for local scientific and technological development guided by the central government in 2023 from Tibet Science and Technology Department (NO. XZ202301YD0014C), the Major science and technology research project in 2023 from Tibet Science and Technology Department (NO. XZ202301ZY0009G), the Key support projects of the central government for local transfer payment funds (inheritance and development of traditional Chinese medicine) in the Xizang Autonomous Region in 2023 (NO. 2023-XZ-ZYYJ-01-LH).

Disclosure

The authors declare that they do not have any conflict of interest.

References

1. Cao X, Wang Y, Chen Y, et al. Advances in traditional Chinese medicine for the treatment of chronic obstructive pulmonary disease. *J Ethnopharmacol*. 2023;307:116229. doi:10.1016/j.jep.2023.116229
2. Kathrin K, Rudolf AJ, Jürgen B, et al. The diagnosis and treatment of COPD and its comorbidities. *Dtsch Arztebl Int*. 2023;120:434–444. doi:10.3238/arztebl.m2023.027
3. Li LY, Zhang CT, Zhu FY, et al. Potential natural small molecular compounds for the treatment of chronic obstructive pulmonary disease: an overview. *Front Pharmacol*. 2022;13:821941. doi:10.3389/fphar.2022.821941
4. Christenson SA, Smith BM, Bafadhel M, et al. Chronic obstructive pulmonary disease. *Lancet*. 2022;399(10342):2227–2242. doi:10.1016/s0140-6736(22)00470-6
5. Holtjer JCS, Bloemsma LD, Beijers RJHCG, et al. Identifying risk factors for COPD and adult-onset asthma: an umbrella review. *Eur Respir Rev*. 2023;32(168):230009. doi:10.1183/16000617.0009-2023
6. Barnes Peter J. Cellular and molecular mechanisms of asthma and COPD. *Clin Sci*. 2017;131(13):1541–1558. doi:10.1042/cs20160487
7. Lange P, Ahmed E, Lahmar ZM, et al. Natural history and mechanisms of COPD. *Respirology*. 2021;26(4):298–321. doi:10.1111/resp.14007
8. Wang C, Zhou J, Wang J, et al. Progress in the mechanism and targeted drug therapy for COPD. *Signal Transduction Tar*. 2020;5(1):248. doi:10.1038/s41392-020-00345-x
9. Mintz M, Barjaktarevic I, Mahler DA, et al. Reducing the risk of mortality in chronic obstructive pulmonary disease with pharmacotherapy: a narrative review. *Mayo Clin Proc*. 2023;98(2):301–315. doi:10.1016/j.mayocp.2022.09.007
10. Singh D. Pharmacological treatment of stable chronic obstructive pulmonary disease. *Respirology*. 2021;26(7):643–651. doi:10.1111/resp.14046
11. MacLeod M, Papi A, Contoli M, et al. Chronic obstructive pulmonary disease exacerbation fundamentals: diagnosis, treatment, prevention and disease impact. *Respirology*. 2021;26(6):532–551. doi:10.1111/resp.14041
12. Ferrera MC, Labaki WW, Han MK. Advances in chronic obstructive pulmonary disease. *Ann Rev Med*. 2021;72(1):119–134. doi:10.1146/annurev-med-080919-112707
13. Liapikou A, Antoni TMFT, Torres A. Managing the safety of inhaled corticosteroids in COPD and the risk of pneumonia. *Expert Opin Drug Saf*. 2015;14(8):1237–1247. doi:10.1517/14740338.2015.1057494
14. Larry ETMD. Anticholinergic effects of medication in elderly patients. *J Clin Psychiatr*. 2001;62(Suppl 21):11–14.
15. Billington CK, Penn RB, Hall IP. β2 agonists. *Handb Exp Pharmacol*. 2017;237(237):23–40. doi:10.1007/164.2016.64
16. Milara J, Peiró T, Serrano A, et al. Epithelial to mesenchymal transition is increased in patients with COPD and induced by cigarette smoke. *Thorax*. 2013;68(5):410–420. doi:10.1136/thoraxjnl-2012-201761
17. Shaykhiev R, Crystal RG. Early events in the pathogenesis of chronic obstructive pulmonary disease. Smoking-induced reprogramming of airway epithelial basal progenitor cells. *Ann Am Thorac Soc*. 2014;11(Suppl 5):S252–S258. doi:10.1513/AnnalsATS.201402-049AW
18. Wang Q, Wang Y, Zhang Y, et al. Involvement of urokinase in cigarette smoke extract-induced epithelial-mesenchymal transition in human small airway epithelial cells. *Lab Invest*. 2015;95(5):469–479. doi:10.1038/labinvest.2015.33
19. Guan R, Wang J, Cai Z, et al. Hydrogen sulfide attenuates cigarette smoke-induced airway remodeling by upregulating SIRT1 signaling pathway. *Redox Biol*. 2020;28:101356. doi:10.1016/j.redox.2019.101356
20. Hogg JC, Paré PD, Hackett TL. The contribution of small airway obstruction to the pathogenesis of chronic obstructive pulmonary disease. *Physiol Rev*. 2017;97(2):529–552. doi:10.1152/physrev.00025.2015
21. Chen Y, Guo S, Guan Y, et al. The research progress of medicinal plants fritillaria. *Mol Plant Breed*. 2019;17(18):6198–6206. doi:10.13271/j.mpb.017.006198
22. Jin X, Li C, Zhang H. Research progress on chemical constituents and pharmacological activities of alkaloids in Fritillaria. *J Chinese Med Mater*. 2022;45(09):2273. doi:10.13863/j.issn1001-4454.2022.09.044
23. An Y, Wei W, Li H, et al. An enhanced strategy integrating offline superimposed two-dimensional separation with mass defect filter and diagnostic ion filter: comprehensive characterization of steroid alkaloids in Fritillariae Pallidiflorae Bulbus as a case study. *J Chromatogr A*. 2021;1643:462029. doi:10.1016/j.chroma.2021.462029
24. Li X, Luo Y, Geng Z, et al. Determination of 21 inorganic elements in Fritillariae Pallidiflorae Bulbus by ICP-MS. *West China J Pharm Sci*. 2021;36(4):447–452. doi:10.13375/j.cnki.wcjps.2021.04.017
25. Jiao H, Chen X, Hu J, et al. Review on chemical composition and biological activities of Fritillaria Pallidiflora. *Guangdong Chem Ind*. 2023;50(4):92–3+86.
26. Liu S, Yang T, Ming TW, et al. Isosteroid alkaloids with different chemical structures from Fritillariae cirrhosae bulbus alleviate LPS-induced inflammatory response in RAW 264.7 cells by MAPK signaling pathway. *Int Immunopharmacol*. 2020;78:106047. doi:10.1016/j.intimp.2019.106047
27. Liu S, Yang T, Ming TW, et al. Isosteroid alkaloids from Fritillaria cirrhosa bulbus as inhibitors of cigarette smoke-induced oxidative stress. *Fitoterapia*. 2020;140:104434. doi:10.1016/j.fitote.2019.104434
28. Wang D, Du Q, Li H, et al. The isosteroid alkaloid imperialine from bulbs of Fritillaria cirrhosa mitigates pulmonary functional and structural impairment and suppresses inflammatory response in a COPD-like rat model. *Mediators Inflammation*. 2016;2016:1–17. doi:10.1155/2016/4192483
29. Pai M, Erbu A, Wu Y, et al. Total alkaloids of bulbus of Fritillaria cirrhosa alleviate bleomycin-induced inflammation and pulmonary fibrosis in rats by inhibiting TGF-β and NF-κB signaling pathway. *Food Nutr Res*. 2023;67:10292. doi:10.29219/fnr.v67.10292
30. Liu C, Liu S, Tse WT, et al. A distinction between Fritillaria Cirrhosa Bulbus and Fritillaria Pallidiflora Bulbus via LC-MS/MS in conjunction with principal component analysis and hierarchical cluster analysis. *Sci Rep*. 2023;13(1):2735. doi:10.1038/s41598-023-29631-8
31. Murgia N, Gambelunghe A. Occupational COPD-the most under-recognized occupational lung disease? *Respirology*. 2022;27(6):399–410. doi:10.1111/resp.14272
32. Sokar SS, Afify EH, Osman EY. Dexamethasone and losartan combination treatment protected cigarette smoke-induced COPD in rats. *Hum Exp Toxicol*. 2020;40(2):284–296. doi:10.1177/0960327120950012
33. Yang T, Wang H, Li Y, et al. Serotonin receptors 5-HTR2A and 5-HTR2B are involved in cigarette smoke-induced airway inflammation, mucus hypersecretion and airway remodeling in mice. *Int Immunopharmacol*. 2020;81:106036. doi:10.1016/j.intimp.2019.106036

34. Zhang Q, Yan L, Lu J, et al. Glycyl-L-histidyl-L-lysine-Cu2+ attenuates cigarette smoke-induced pulmonary emphysema and inflammation by reducing oxidative stress pathway. *Front Mol Biosci*. 2022;9:925700. doi:10.3389/fmolb.2022.925700
35. Jain S, Durugkar S, Saha P, et al. Effects of intranasal azithromycin on features of cigarette smoke-induced lung inflammation. *Eur J Pharmacol*. 2022;915:174467. doi:10.1016/j.ejphar.2021.174467
36. Saber BGE, Gareeb AIA, Saad HM, et al. COVID-19 and corticosteroids: a narrative review. *Inflammopharmacology*. 2022;30(4):1189–1205. doi:10.1007/s10787-022-00987-z
37. Liu L, Zhang Y, Xu D, et al. Effect of Rehmanniae radix oligosaccharides on pathological changes in peripheral airways of COPD rats. *J Chinese Med Mater*. 2013;36(10):1678–1681. doi:10.13863/j.issn1001-4454.2013.10.041
38. Xu Y, Li J, Lin Z, et al. Isorhamnetin alleviates airway inflammation by regulating the Nrf2/Keap1 pathway in a mouse model of COPD. *Front Pharmacol*. 2022;13:860362. doi:10.3389/fphar.2022.860362
39. Li J, Xie Y, Zhao P, et al. A Chinese herbal formula ameliorates COPD by inhibiting the inflammatory response via downregulation of p65, JNK, and p38. *Phytomedicine*. 2021;83:153475. doi:10.1016/j.phymed.2021.153475
40. Deng M, Tong R, Bian Y, et al. Astaxanthin attenuates cigarette smoking-induced oxidative stress and inflammation in a sirtuin 1-dependent manner. *Biomed Pharmacother*. 2023;159:114230. doi:10.1016/j.biopha.2023.114230
41. Yi X, Li T, Wei X, et al. Erythromycin attenuates oxidative stress-induced cellular senescence via the PI3K-mTOR signaling pathway in chronic obstructive pulmonary disease. *Front Pharmacol*. 2022;13:1043474. doi:10.3389/fphar.2022.1043474
42. Liang S, Zheng Y, Lei L, et al. Corydalis edulis total alkaloids (CETA) ameliorates cognitive dysfunction in rat model of Alzheimer disease through regulation of the antioxidant stress and MAP2/NF-κB. *J Ethnopharmacol*. 2020;251:112540. doi:10.1016/j.jep.2019.112540
43. Lai T, Li Y, Chen M, et al. Heparin-binding epidermal growth factor contributes to COPD disease severity by modulating airway fibrosis and pulmonary epithelial–mesenchymal transition. *Lab Invest*. 2018;98(9):1159–1169. doi:10.1038/s41374-018-0049-0
44. Wang Q, Sundar IK, Lucas JH, et al. Molecular clock REV-ERBα regulates cigarette smoke–induced pulmonary inflammation and epithelial-mesenchymal transition. *JCI Insight*. 2021;6(12):145200. doi:10.1172/jci.insight.145200
45. Jiang B, Guan Y, Shen H, et al. Akt/PKB signaling regulates cigarette smoke-induced pulmonary epithelial-mesenchymal transition. *Lung Cancer*. 2018;122:44–53. doi:10.1016/j.lungcan.2018.05.019
46. Mahmood MQ, Reid D, Ward C, et al. Transforming growth factor (TGF) β1 and Smad signalling pathways: a likely key to EMT-associated COPD pathogenesis. *Respirology*. 2016;22(1):133–140. doi:10.1111/resp.12882
47. Ostridge K, Williams N, Kim V, et al. Distinct emphysema subtypes defined by quantitative CT analysis are associated with specific pulmonary matrix metalloproteinases. *Respir Res*. 2016;17(1):92–100. doi:10.1186/s12931-016-0402-z
48. Li C, Huang Z, Li W, et al. The nucleotide-binding oligomerization domain–like receptor family pyrin domain-containing 3 inflammasome regulates bronchial epithelial cell injury and proapoptosis after exposure to biomass fuel smoke. *Am J Resp Cell Mol*. 2016;55(6):815–824. doi:10.1165/rcmb.2016-0051OC
49. Tao Y, Sun Y, Wu B, et al. Overexpression of FOXA2 attenuates cigarette smoke-induced cellular senescence and lung inflammation through inhibition of the p38 and Erk1/2 MAPK pathways. *Int Immunopharmacol*. 2021;94:107427. doi:10.1016/j.intimp.2021.107427
50. Pelaia C, Vatrella A, Gallelli L, et al. Role of p38 mitogen-activated protein kinase in asthma and COPD: pathogenic aspects and potential targeted therapies. *Drug Des Dev Ther*. 2021;15:1275–1284. doi:10.2147/dddt.S300988
51. Guan R, Wang J, Li Z, et al. Sodium tanshinone IIA sulfonate decreases cigarette smoke-induced inflammation and oxidative stress via blocking the activation of MAPK/HIF-1α signaling pathway. *Front Pharmacol*. 2018;9:1–13. doi:10.3389/fphar.2018.00263
52. Guan R, Wang J, Li D, et al. Hydrogen sulfide inhibits cigarette smoke-induced inflammation and injury in alveolar epithelial cells by suppressing PHD2/HIF-1α/MAPK signaling pathway. *Int Immunopharmacol*. 2020;81:105979. doi:10.1016/j.intimp.2019.105979
53. Bin YF, Ma N, Lu YX, et al. Erythromycin reverses cigarette smoke extract-induced corticosteroid insensitivity by inhibition of the JNK/c-Jun pathway. *Free Radic Biol Med*. 2020;152:494–503. doi:10.1016/j.freeradbiomed.2019.11.020